Am J Transl Res 2022;14(6):3806-3823
www.ajtr.org /ISSN:1943-8141/AJTR0135208

Original Article

The expression profile of plasmatic exosomal lncRNAs in early-onset preeclampsia by sequencing

Xiaoqian Fu*, Min Wu*, Yue Chen, Liling Li, Hongyu Yin, Kaili Liang, Yachang Zeng

*Department of Obstetrics and Gynecology, The First Affiliated Hospital of Guangxi Medical University, Nanning 530021, Guangxi, China. *Equal contributors.*

Received May 13, 2021; Accepted May 5, 2022; Epub June 15, 2022; Published June 30, 2022

Abstract: Identification of the expression profile of exosomal lncRNAs in plasma from PE patients to provide new insights into the molecular mechanism. Five pregnant patients with early-onset severe PE were included in the PE group and 5 normal pregnant patients were included in the control group in the training cohort. Differential expression of genes were identified between the two groups, and were verified in plasma exosomes from 12 additional pregnant patients with EPE and 12 normal pregnant patients. KEGG pathway analysis and GO enrichment analysis were performed using online prediction databases to construct a lncRNA-miRNA-mRNA co-expression network. From there a panel of candidate lncRNAs was selected and validated via quantitative PCR in the two groups. In the 289 differential lncRNA, 155 were up-regulated and 134 were down-regulated. Bioinformatics enrichment analysis demonstrated that the target genes of differential expression of lncRNAs were enriched in 159 pathways with $P < 0.05$, including cancer, metabolic and PI3K-Akt signaling pathways. Three lncRNAs exhibited significant differential expressed in exosomes between the two groups. A lncRNA-miRNA-mRNA co-expression network analysis showed that ENST00000559730-hsa-miR-661-NUDT16 was the most frequently associated with susceptibility-relation of PE. The significant differences of plasmatic exosomal lncRNA expression between normal pregnant women and early-onset severe PE patients suggest that lncRNA may participate in the pathogenetic process of PE. Our study provides a preliminary bioinformatic foundation in order to find PE markers in plasma which further increase the sample size, and continue to verify the function of lncRNA *in vitro*.

Keywords: Preeclampsia, exosome, long non-code RNA (lncRNA), miRNA, PI3K-Akt

Introduction

Preeclampsia (PE) is a common gestational complication and manifests as new-onset hypertension, proteinuria, placental, and organ dysfunction, commonly occur after 20 weeks of gestation. PE is one of the main cause of maternal and neonatal morbidity and mortality, and affects approximately 5-8% of pregnant women around the world [1]. Although extensive studies have been conducted from various angles, the pathogenesis and etiology of PE is still not clear. Currently, the occurrence of PE is considered to be related to maternal endothelial dysfunction, uterine spiral artery remodeling dysfunction and abnormal placental implantation. Placental dysfunction may explain the main pathologic features associated with the complications. Early-onset preeclampsia which is considered as a placental disease mainly affects both mother and fetus due to placental abnormity, while late-onset preeclampsia may be caused by the synergy of placental degeneration and the genetic susceptibility to cardiovascular and metabolic diseases [2].

The placental cell-derived exosomes secreted into the maternal circulation regulates the function of maternal organs, establishes the communication between mother and fetus, and accommodates the demands for maintaining pregnancy and its plasma concentration is 50 times that in non-pregnant women [3]. Exosomes are membrane-derived extracellular vesicles (EVs) released by a variety of cell types that deliver bioactive substances, such as protein, lncRNA, miRNA, and lipids to mediate cell-cell communication [4]. Recent studies have found that the changes in protein, lncRNA and other content of placenta derived exosomes

affect trophoblast function, angiogenesis or other aspects, which may be related to pathological pregnancy such as preeclampsia [4, 5]. At present, most studies focus on the role of exosomal lncRNA in placenta or decidua, but few studies have been conducted on plasmatic lncRNA [6-8].

With the development of sequencing technology, it has been found that a variety of lncRNA are abnormally expressed in the placenta of PE patients. Further silencing/overexpression tests show that lncRNA can change trophoblast function, participate in immune regulation, epigenetic regulation, decidualization and other aspects. Most of these studies focus on the analysis of lncRNA in placental samples, and most of them are *in vitro* experiments, and no consensual conclusion has been reached. Wang et al. proposed that the regulatory network in psg10p/mir-19a-3p/IL1RAP pathway may be involved in the pathogenesis of PE [9]. Wu et al. hypothesized that MALAT1 could regulate the migration and invasion of trophoblast cells through PI3K-Akt signaling pathway by regulating miR-206/IGF-1 axis [10]. However, changes in the expression levels of multiple lncRNAs may lead to the same phenotype, while changes in the expression of a single lncRNA may lead to cell phenotype due to its involvement in a variety of biological pathways. Whether the change of lncRNA expression is a cause or a result needs to be determined by further clarification of the regulatory mechanism at the molecular level.

However, it is difficult to obtain placental tissues before parturition. Furthermore, biological fluids such as blood, urine and saliva are much easier to obtain and may be more clinically practical in prenatal screening and diagnosis. In this study, we detected the expression profile difference of plasmatic exosomal lncRNA between early-onset severe PE patients and normal pregnant women by high-throughput RNA sequencing and provided evidence for their biologic activity in the pathogenesis of PE.

Material and methods

Patients

Five pregnant women with early-onset severe PE who delivered in the First Affiliated Hospital of Guangxi Medical University from June to November 2019 were included in the experimental group (PE group) in the training cohort, and twelve pregant women with early-onset severe PE collected from May to September 2021 were included in the PE group in the validation cohort. A diagnosis of early-onset severe PE was made when a singleton pregnant woman presented with a systolic blood pressure ≥ 140 mmHg or/and diastolic blood pressure ≥ 90 mmHg before 34 weeks' gestation with one or more severe complication(s) which was defined by Oxford Textbook of Obstetrics and Gynaecology [11]. The control group (NC group) in training cohort recuited 5 normal pregnant women who were acceptedwith routine prenatal examination in the First Affilicated Hospital of Guangxi Medical University in the same period as well as 12 normal pregant women in validation cohort in the same period of PE group in validation cohort. All the pregnant woman including thoes with PE and in the NC group who met the following criteria were excluded: 1. Age ≥ 40 or ≤ 18 years old, BMI ≥ 30 kg/m^2, history of gestational hypertension, preeclampsia or family history were excluded; 2. Diabetes mellitus, cardiovascular disease, blood system disease, liver and kidney disease and other medical complications; 3. Intrahepatic cholestasis, gestational diabetes mellitus, and acute fatty liver; 4. Multiple pregnancies, fetal abnormalities, premature rupture and intrauterine infection. In this study, the diagnosis of Early-onset Preeclampsia was defined as 34 weeks ago according to Oxford Textbook of Obstetrics and gynaecology. Previous studies have found that the concentration of exosomes of pregnant women with different gestational weeks has great differences [3], and the number of cases in this study is small. In order to avoid the influence of gestational weeks on the results, the sample collection time is concentrated in 28-35 weeks. The patients in this study all did not define the number of births. This study was approved by the ethics committee of Guangxi Medical University and conducted following the ethical standards of the responsible committee on human experimentation (institutional and national) and with the Helsinki Declaration of 1975, as revised in 2008. The study participants gave informed consent for genetic analysis before inclusion.

Plasma collection and exosomes isolation

Methods of plasma collection, exosome extraction and identification were from ISEV stan-

dards [12, 13]. At the 28th to 35th week of pregnancy, 15 ml blood samples from the peripheral blood of each participant in the two cohorts were collected in EDTA-K2 tubes. The collected blood sample was allowed to stand at 4°C for 3 to 4 hours, followed by centrifugation at 4000 × g for 5 minutes at 4°C. Subsequently, the resulting supernatant was collected. The exosomes were separated from the plasma using precipitation separation method. The plasma was first centrifuged at 2000 g for 20 min at 4°C to spin down blood cells and fragments. Supernatants were placed into 3:1 (v/v) RiboTM exosome Isolation reagent (RiboBio, China) and mixed. Setting for 30 min at 4°C, centrifuged at 15,000 g for 2 min at 4°C to spin down the exosomes [14].

Transmission electron microscopy

A volume of 1 μL of exosomes was placed on a 400-mesh copper grid and incubated for 1 min at room temperature, followed by incubation with 20 g/l phosphotungstic acid (pH = 6.8) for 1 min. The grid was dried at 37°C for 15 min and was then observed using H-7650 transmission electron microscopy (TEM) (Hitachi, Japan).

Flow cytometry

To confirm the extracellular vesicles types, isolated particles were stained with the Fluorescein thiocyanate (FITC)-conjugated anti-CD63, and PE-conjugated anti-CD81. The stained exosome particles were evaluated using BD Accuri C6 flow cytometer and statistically analyzed using FlowJo V10 software.

Nanoparticle tracking analysis

ZETASIZER Nano series-Nano-ZS (NanoSight Technology, UK) was used to measure the proportion of exosomes. Exosomes were resuspended in 1 ml PBS. Samples were injected into the sample chamber at room temperature. All operating procedures followed the instrument manufacturer's instruction. Finally, the results were analyzed using nanoparticle tracking analysis software.

Western blotting

Total protein was extracted from exosomes. Anti-CD63 (SBI, USA, 1:1000), Anti-TSG101 (SBI, USA, 1:1000), Anti-rabbit IgG, HRP-linked Antibody (SBI, USA). Protein concentration was measured using the BCA protein assay kit. Sodium dodecyl sulfate-polyacrylamide gel electrophoresis was used to separate lysates, followed by protein transfer using PVDF membranes. After incubation with antibodies, the target bands were detected using E3 imaging system.

Total RNA extraction

The total RNA from the exosomes was subjected to biochemistry and molecular biology by Trizol (Invitrogen) according to the protocol instructions. The total RNA was separated from exosome suspension and eluted by RNase-free water. Subsequently, a 1 μL RNA solution was quantified using Nanodrop (Thermo Scientific). Finally, the total RNA samples were stored at -80°C.

Construction of cDNA library and lncRNA sequencing

cDNA was synthesized according to the instructions provided by the kit (NEB, USA) and the purity of cDNA was evaluated using Agilent 2200 TapeStation (Life Technologies, USA). LncRNA sequencing was performed in Guangzhou RiboBio Co., Ltd. (Guangzhou, China), using the Illumina HiSeq 3000 platform for paired-end sequencing (PE150, Sequencing reading were 150 bp). The original fastq sequence was processed using TRAILING: 20, MINLEN: 235, and CROP: 235, followed by Trimmomatic tools (v0.36) to remove trailing sequences with a mass score below 20, and to obtain a uniform sequence length for the downstream clustering process. Paired-end reading were aligned to reference human genome hg19 with HISAT2. HTSeq v0.6.0 was used to count the reading numbers mapped to each gene. The whole samples expression levels were presented as RPKM (expected number of Reads PerKilobase of transcript sequence per Million base pairssequenced), which is the recommended and most common method to estimate the level of gene expression. The statistically significant DE genes were obtained by an adjusted *P*-value threshold of < 0.05 and $|\log2(\text{fold change})| > 1$ using the DEGseq software. Finally, a hierarchical clustering analysis was performed using the R language package gplots according to the RPKM values of differential genes in different groups. Different clustering information was represented in colors, such as the similar expression pattern in the same group, including similar functions or inclusion in the same biological process.

Table 1. Primers used in analysis of lncRNAs expression by qRT-PCR

lncRNA	Forward	Reward
ENST00000559730.1	CACACTGTTCTGGTCCTGATGTC	GCTCTGGGAATGAGGTGCTT
ENST00000428958.1	GCCATCTGTCTCTTTGCCTCA	CAACTGCACCCATTCTCCTG
ENST00000573220.1	AGTGACTTGCCATTGAGTCCG	CCGATAACTGAGGGCAGCAG

lncRNA target prediction

The relationship between the predicted potential target genes of aberrantly expressed lncRNAs and the aberrantly expressed mRNAs was examined. To determine the functions of lncRNAs in the regulation of target gene expression in cis and in trans. The differential expression of lncRNA and mRNA were sequenced to estimate trans regulation followed by preliminarily screening using Blast software (e < 1E-5) and RNAplex software was used for further screening to identify potential target genes of lncRNA.

GO function and KEGG pathway enrichment analysis

All differential expression of mRNAs were selected for GO analysis and KEGG pathway analysis. GO was performed with KOBAS3.0 software. GO provides label classification of gene function and gene product attributes (http://www.geneontology.org). GO analysis includes: cellular component (CC), molecular function (MF) and biological process (BP). The differential expression of mRNAs and the enrichment of different pathways were mapped by KEGG pathways using KOBAS3.0 software (http://www.genome.jp/kegg).

Candidate lncRNAs validation

Exosomal RNA extraction and quantification were performed as aforementioned. cDNA was generated using C1000 Touch (Bio-Rad, USA) according to the manufacturer's instructions. Quantitative real-time PCR was performed on the CFX Connect (Bio-Rad, USA) using primers specific for ENST00000559730.1, ENST00000428958.1 and ENST00000573220.1 which were synthesized by Guangzhou RiboBio Co., Ltd. (Guangzhou, China). All primers used in this study are listed in **Table 1**. The reaction system was established as follows: 2 × SYBR green mix 5 μL, forward primer (10 μm) 0.4 μL, reverse primer (10 μm) 0.4 μL, cDNA 2 μL, RNase free H_2O 2.2 μL, total 10 μL. PCR amplification was carried out according to the following procedures: 95°C for 10 min, * 95°C for 10 s, 60°C for 20 s, 70°C for 10 s, read the plate, return * for 40 cycles, and the melting curve was made: between 70°C and 95°C, each time Read the board at 0.5°C for 5 seconds. The specificity of amplification was confirmed by calculating melting curve profiles at the end of each PCR analysis. Each sample was analyzed in triplicate.

lncRNA-miRNA-mRNA co-expression network construction

To determine the function of aberrantly expressed lncRNAs in PE, the key lncRNA, miRNA and mRNA were screened through the quantitative relationship in the network, which laid a bioinformatics foundation for the subsequent co-expression verification experiments. The co-expression network was constructed by calculating the Pearson correlation coefficient and *P* value between multiple genes. In our study, the transcripts were filtered using a |log2 (Fold Change)| > 1 and a *P*-value of < 0.05. Furthermore, we selected 3 DE mRNA transcripts that were enriched in reproduction-related pathways and all DE lncRNAs to construct a co-expression network, the co-expression network was illustrated on the cytohubba plug-in (package) in Cytoscape 3.7.0 software, the key nodes and subnetworks in the network are predicted by degree topology algorithm.

Statistical analysis

All results in this study are represented by the mean ± SD and the comparisons were performed using T-test and one-way ANOVA by SPSS 20.0 software. Accordingly, *P*-values of < 0.05 were considered statistically significant.

Results

Patient characteristics

In this study, baseline characteristics, such as age, BMI bleeding gestational age, between

Table 2. Basic characteristics of the subjects

	Training cohort		Validation cohort	
	PE group	NC group	PE group	NC group
Age (years)	32.20 ± 3.96	28.80 ± 3.19	31.58 ± 4.46	30.67 ± 4.52
BMI (kg/m^2)	25.32 ± 3.38	24.79 ± 2.59	23.67 ± 3.35	24.01 ± 3.99
Bleeding Gestational Age (weeks)	34.29 ± 2.01	34.69 ± 0.47	31.45 ± 3.30	35.70 ± 2.16

The comparisons were performed using independent-sample t test by SPSS 22.0 software (SPSS, Chicago, IL, USA). *P*-values of < 0.05.

the two groups showed no statistical significance. The clinical indications of the PE patients are listed in **Table 2**. In the NC group, there was no occurance of complications during pregnancy, such as preterm delivery, late-onset preeclampsia, etc. In the PE group, all pregnancies were terminated by cesarean section. The duration of termination was 28 weeks to 36+3 weeks, in which there were 2 cases of fetal distresswhich comprise of 1 case of severe neonatal asphyxia, furthermore, there were no cases of placental abruption, eclampsia, HELLP syndrome, maternal or perinatal death, and postpartum hemorrhage. In the NC group, the duration of termination of pregnancy was 35+4 weeks to 40+0 weeks, there are no occurance of fetal distress, neonatal asphyxia, postpartum hemorrhage, maternal or perinatal death. In the validation experiment of lncRNA, we used new cases, including 12 cases in PE group and 12 cases in NC group. The inclusion criteria were the same as those of the previous experimental group. Basic characteristics of the subjects for validation are summarized in **Table 2**.

Characterization of plasma exosomes

Exosomes were isolated and purified from the plasma of PE patients and NC subjects and were observed using a TEM. Typicle dent hemisphere-like structure with a double-layer capsule were observed (**Figure 1A**). ZETASIZER Nano analysis showed the detected particle distribution coefficient (PDI) was between 0.08 and 0.7, the average particle diameter is 57.04 nm and the size distribution was mainly between 20 and 200 nm which percentage is 86.4% (**Figure 1B**). It is indicated that the dispersion degree of the system is moderate and the test results is reliable. Results of flow cytometry showed the CD63 and CD81 expression of the particles are 82.5% and 86.7% represently (**Figure 1C**). The extracted exosomal RNAs were inspected, and the results showed that the RNAs were in good quality and met the sequencing requirements (**Figure 1D**). Western blotting analysis of exosomal markers CD63 and TSG101 further confirmed the identity of the exosomes (**Figure 1E**).

Profiles of the aberrantly expressed lncRNAs and lncRNA target prediction

A total of 289 lncRNAs (155 up-regulated and 134 down-regulated) were significantly aberrantly expressed between two groups (**Figure 2A**). The top 10 dis-regulated (up-regulated and down-regulated) lncRNAs were shown in **Figure 2B** and **Table 3**. For the prediction of lncRNAs, the target mRNAs is regulated in cis. The potential mRNA targets were calculated by integrating the differential expression of lncRNA data and its adjacent differential expression of mRNA (10 kb). According to this criteria, 276 lncRNAs were found to have 386 regulatory mRNAs in cis. For the prediction of lncRNAs, the target mRNAs is regulated in trans. The differential expression of lncRNAs and mRNAs were sequenced and preliminarily screened by Blast software (e < 1E-5), and then RNAplex software was used for further screening to identify potential target mRNAs of lncRNA. According to this criteria, 1701 mRNAs were regulated by 138 lncRNAs in trans.

GO enrichment analysis of aberrantly expressed mRNAs

GO enrichment analysis provides three aspects, i.e. molecular function, biological process and cell composition for the target mRNA. Regarding the cell composition, target mRNA were mainly enriched in intracellular, organelles and membrane-bound organelles (**Figure 3A**). In terms of molecular function, the target mRNA were associated with binding, catalytic activity and nucleic acid binding (**Figure 3B**). Regarding the biological process, it mainly concentrates in cell process, metabolic process, biological regulation and other processes (**Figure 3C**).

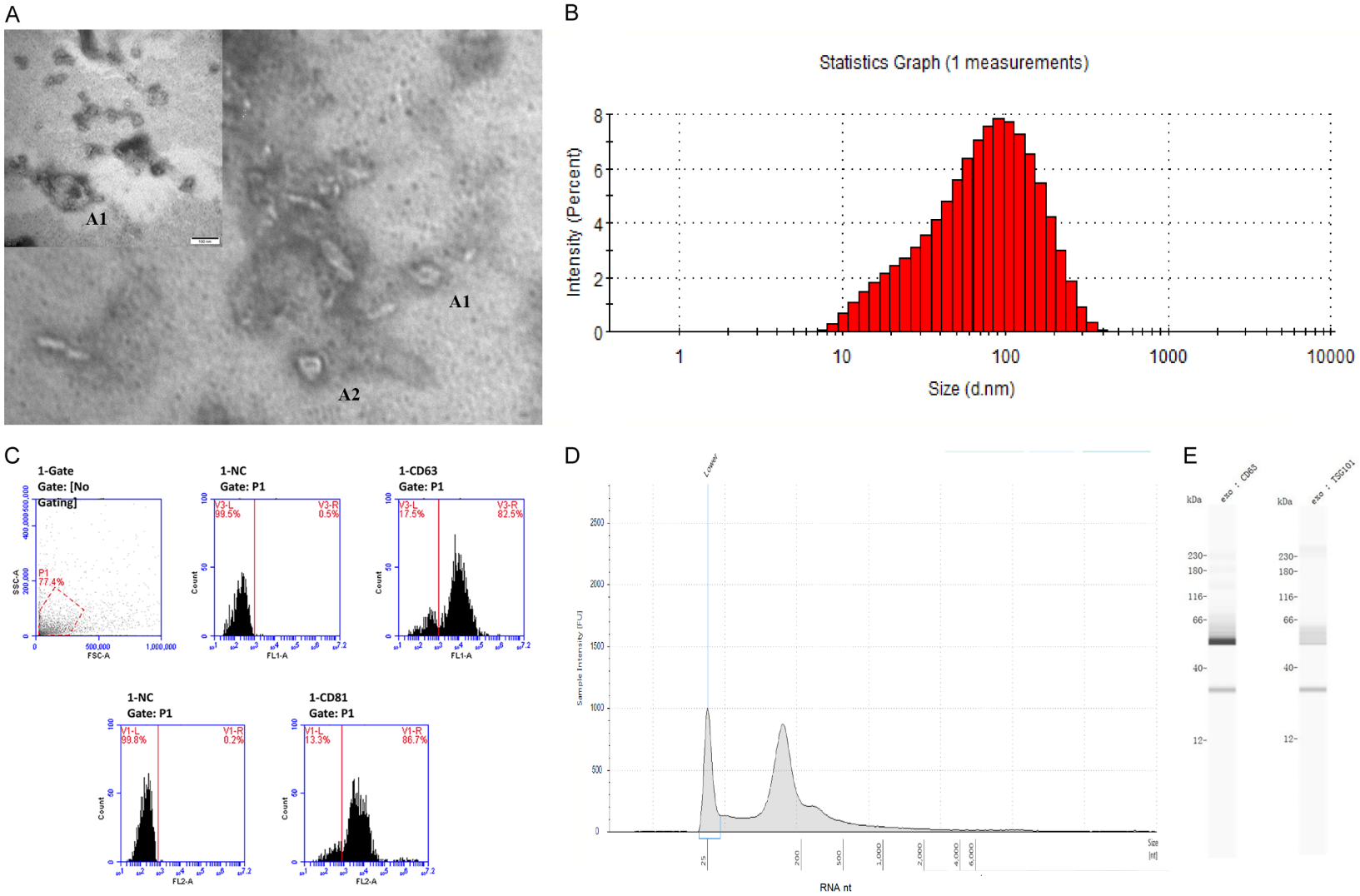

Figure 1. Characteristics of exosomes. A. Representative TEM images of plasma-derived exosomes (100,000-fold). TEM, transmission electron microscopy. Exosomes showed the ultrastructure of dent hemisphere-like structure with a double-layer capsule (A1, A2). B. A result of Nanoparticle tracking analysis to measure the size of exosomes. C. Representative figure of flow cytometry images. In the isolated particles, there were 82.5% and 86.7% particles expressed exosomal special surface marker, CD63 and CD81 respectively. D. The quality check result of extracted exosomal RNAs and it shows RNAs were in good quality. E. Western blots of CD63, and TSG101.

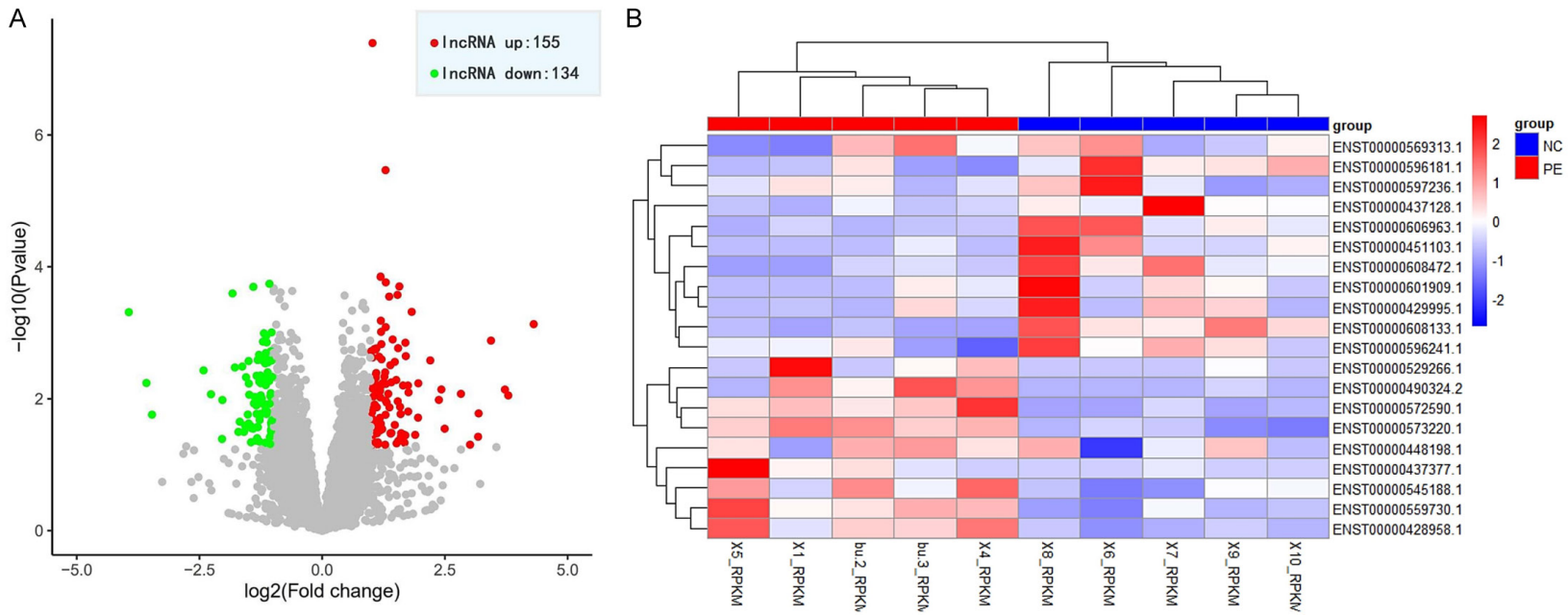

Figure 2. Aberrantly expressed lncRNAs in PE and normal NC samples. A. Volcano plot illustrating differential expression of lncRNAs between PE and NC samples. The abscissa represents the change of the expression multiple of lncRNA in different samples, while the ordinate represents the statistical significance of the difference in gene expression. Up-regulated lncRNAs are denoted in red and down-regulated in green. B. Hierarchically clustered heatmap illustrating the top 10 up-regulated and down- regulated lncRNAs between PE and NC samples. Up-regulated lncRNAs are denoted in red and down-regulated in blue.

Table 3. Top 10 up-regulated and down-regulated lncRNAs (PE vs. NC)

lncRNA	Chromosome position	PE normalize	NC normalize	log2 (Fold change)	*P*-value	Up/ Down	nearest mRNA
ENST00000448198.1	Chromosome 6:32,718,005-32,719,170:+	5.8	0.0	4.96	2.64E-05	Up	HLA-DQA2
ENST00000529266.1	Chromosome 11:112,967-125,927:-	7.4	0.2	4.85	4.98E-05	Up	BET1L
ENST00000559730.1	Chromosome 15:40,464,193-40,466,726:-	35.8	16.0	1.19	1.41E-04	Up	BAHD1
ENST00000573220.1	Chromosome 16:4,180,117-4,183,515:-	24.8	10.2	1.29	1.71E-04	Up	SRL
ENST00000428958.1	Chromosome 9:93,091,406-93,095,710:-	20.6	7.0	1.57	2.00E-04	Up	CARD19
ENST00000545188.1	Chromosome 12:65,622,273-65,663,299:+	26.8	10.8	1.37	2.35E-04	Up	HMGA2
ENST00000437377.1	Chromosome 1:145,827,205-145,833,118:+	3.8	0.2	3.79	9.01E-03	Up	GPR89A
ENST00000596241.1	Chromosome 16: 26,329,428-26,345,749:+	5.6	0.4	3.77	2.96E-03	Up	HS3ST4
ENST00000490324.2	Chromosome 3:101,823,793-101,824,998:-	3.6	0.2	3.72	7.58E-03	Up	NXPE3
ENST00000572590.1	Chromosome 17:81,461,013-81,461,937:-	6.4	0.6	3.44	1.37E-03	Up	ACTG1
ENST00000608133.1	Chromosome 3:175,527,552-175,528,340	0.4	6.4	-3.94	4.89E-04	Down	NAALADL2
ENST00000608472.1	Chromosome 3:139,349,024-139,349,371:-	1.4	7.2	-2.42	3.67E-03	Down	MRPS22
ENST00000451103.1	Chromosome 7: 62,854,655-62,855,817:+	0.4	4.6	-3.58	5.77E-03	Down	VN1R32P
ENST00000437128.1	Chromosome 1:89,260,582-89,269,754:+	1.4	6.8	-2.27	8.46E-03	Down	GBP5
ENST00000606963.1	Chromosome 8:65,591,850-65,592,472:-	1.6	6.4	-2.04	1.04E-02	Down	ARMC1
ENST00000569313.1	Chromosome 5:43,287,601-43,290,839:+	0.4	4.2	-3.43	1.10E-02	Down	HMGCS1
ENST00000597236.1	Chromosome 1:146,093,234-146,159,103:-	0.4	3.6	-3.3	3.10E-02	Down	NBPF11
ENST00000596181.1	Chromosome 1:146,093,234-146,159,103:-	0.4	3.4	-3.21	3.76E-02	Down	NBPF11
ENST00000429995.1	Chromosome 22: 20,336,866-20,341,114:-	1.2	5.6	-2.32	3.89E-02	Down	DGCR6L
ENST00000601909.1	Chromosome 1:151,798,054-151,798,602:+	1.8	6.6	-2.03	4.10E-02	Down	LINGO4

KEGG pathway enrichment analysis

The KEGG pathway analysis provided the annotation information of the signaling transduction pathway for the target mRNA and the distribution information of significant gene sets in the KEGG category. The results showed that the predicted target mRNAs of lncRNA were mainly involved in the metabolic pathway, cell cycle, and PI3K-Akt signaling pathway (Background number: 342, P = 0.000248) (**Figure 4**).

Candidate lncRNAs validation

Three candidate lncRNAs were selected from the training cohort on the basis of the difference multiple (|log2 (Fold Change)| > 1) and significance level (P < 0.05) (**Figure 5A**). Exosomal lncRNAs were verified in 12 cases in PE group and NC group in validation cohort respectively. qRT-PCR results showed that lncRNA ENST00000559730.1, lncRNA ENST00000428958.1 and lncRNA ENST00000573220.1 exhibited higher expression in PE group than in NC group (**Figure 5B**). The qRT-PCR results validated the lncRNA expressions associated with PE pathogenesis.

lncRNA-miRNA-mRNA network

The lncRNA-miRNA network indicates the relationships between aberrantly expressed lncRNA and its potential target miRNAs using miRcode software. Three out of the aforementioned miRNAs were significant abberant expression in PE (**Figure 6A**). The lncRNA-miRNA co-expression network (Top 5) were established using database screening, literature review and data analysis (**Figure 6B**). **Figure 6C** showed the strongest correlation of these networks which was ENST00000559730-hsa-miR-661-NUDT16.

Discussion

Uterine spiral artery remodeling is insufficient in PE patients thus results in decreased placental perfusion, especially in early-onset PE [15]. Therefore, patients with early-onset severe preeclampsia are suitable for this study. It is reported that exosomes isolated from maternal plasma and serum contain placental DNA, the detected exosome-associated DNA concentration in plasma is significantly higher than that in serum [16]. At the same time, with the rapid development of the lncRNA research field, many studies have shown that lncRNA might be involved in the occurrence and development of PE via multiple mechanisms, such as altering trophoblast cell function, regulating the immune system, and epigenetics, effecting decidualization [17]. Although the exact functions of most lncRNAs are still unknown, the function of lncRNA will be meaningful to explore the patho-

A

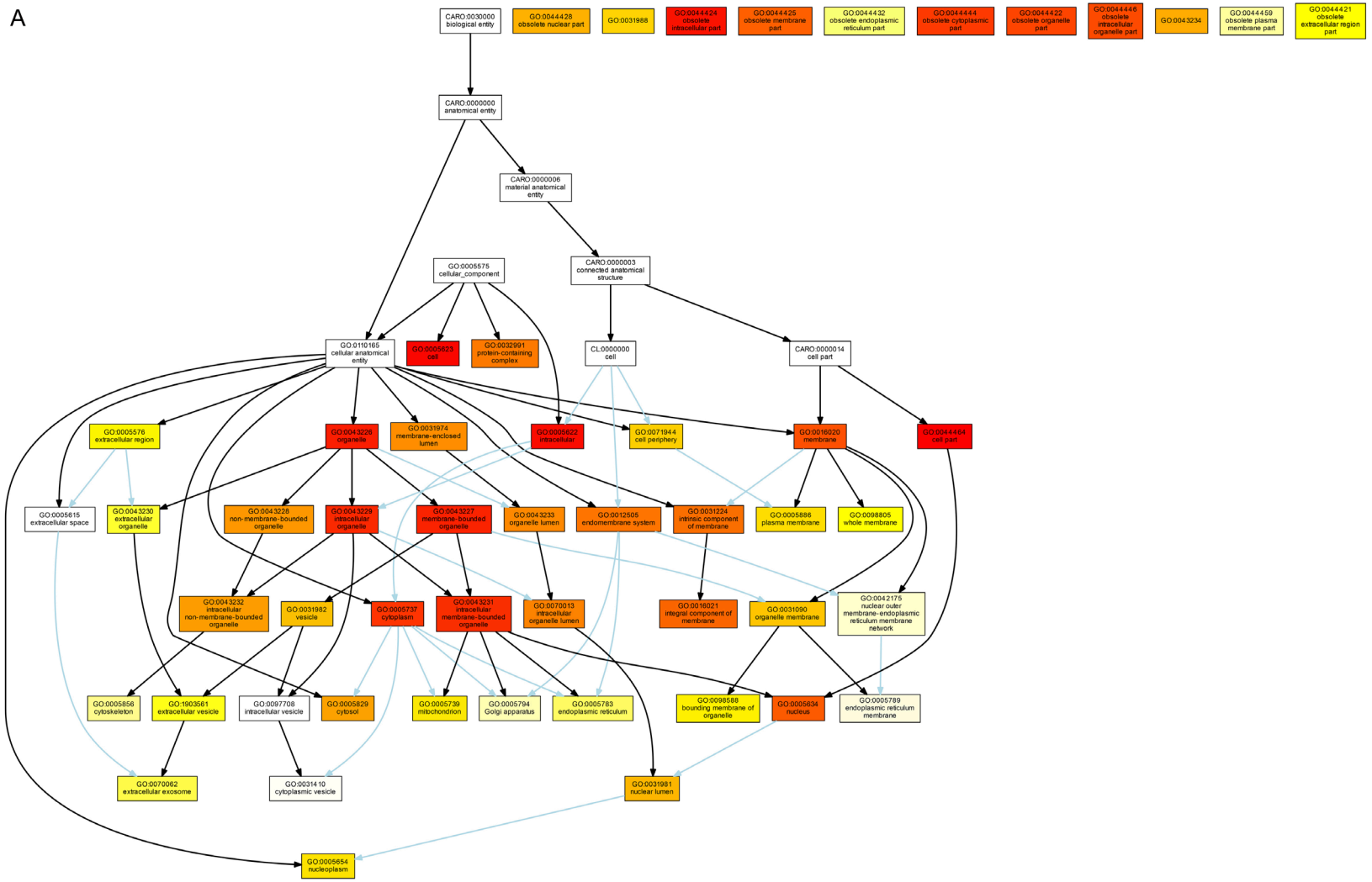
CARO:0030000 biological entity
GO:0044428 obsolete nuclear part
GO:0031988
GO:0044424 obsolete intracellular part
GO:0044425 obsolete membrane part
GO:0044432 obsolete endoplasmic reticulum part
GO:0044444 obsolete cytoplasmic part
GO:0044422 obsolete organelle part
GO:0044446 obsolete intracellular organelle part
GO:0043234
GO:0044459 obsolete plasma membrane part
GO:0044421 obsolete extracellular region part
CARO:0000000 anatomical entity
CARO:0000006 material anatomical entity
GO:0005575 cellular_component
CARO:0000003 connected anatomical structure
GO:0110165 cellular anatomical entity
GO:0005623 cell
GO:0032991 protein-containing complex
CL:0000000 cell
CARO:0000014 cell part
GO:0005576 extracellular region
GO:0043226 organelle
GO:0031974 membrane-enclosed lumen
GO:0005622 intracellular
GO:0071944 cell periphery
GO:0016020 membrane
GO:0044464 cell part
GO:0005615 extracellular space
GO:0043230 extracellular organelle
GO:0043228 non-membrane-bounded organelle
GO:0043229 intracellular organelle
GO:0043227 membrane-bounded organelle
GO:0043233 organelle lumen
GO:0012505 endomembrane system
GO:0031224 intrinsic component of membrane
GO:0005886 plasma membrane
GO:0098805 whole membrane
GO:0043232 intracellular non-membrane-bounded organelle
GO:0031982 vesicle
GO:0005737 cytoplasm
GO:0043231 intracellular membrane-bounded organelle
GO:0070013 intracellular organelle lumen
GO:0016021 integral component of membrane
GO:0031090 organelle membrane
GO:0042175 nuclear outer membrane-endoplasmic reticulum membrane network
GO:0005856 cytoskeleton
GO:1903561 extracellular vesicle
GO:0097708 intracellular vesicle
GO:0005829 cytosol
GO:0005739 mitochondrion
GO:0005794 Golgi apparatus
GO:0005783 endoplasmic reticulum
GO:0098588 bounding membrane of organelle
GO:0005634 nucleus
GO:0005789 endoplasmic reticulum membrane
GO:0070062 extracellular exosome
GO:0031410 cytoplasmic vesicle
GO:0031981 nuclear lumen
GO:0005654 nucleoplasm

B

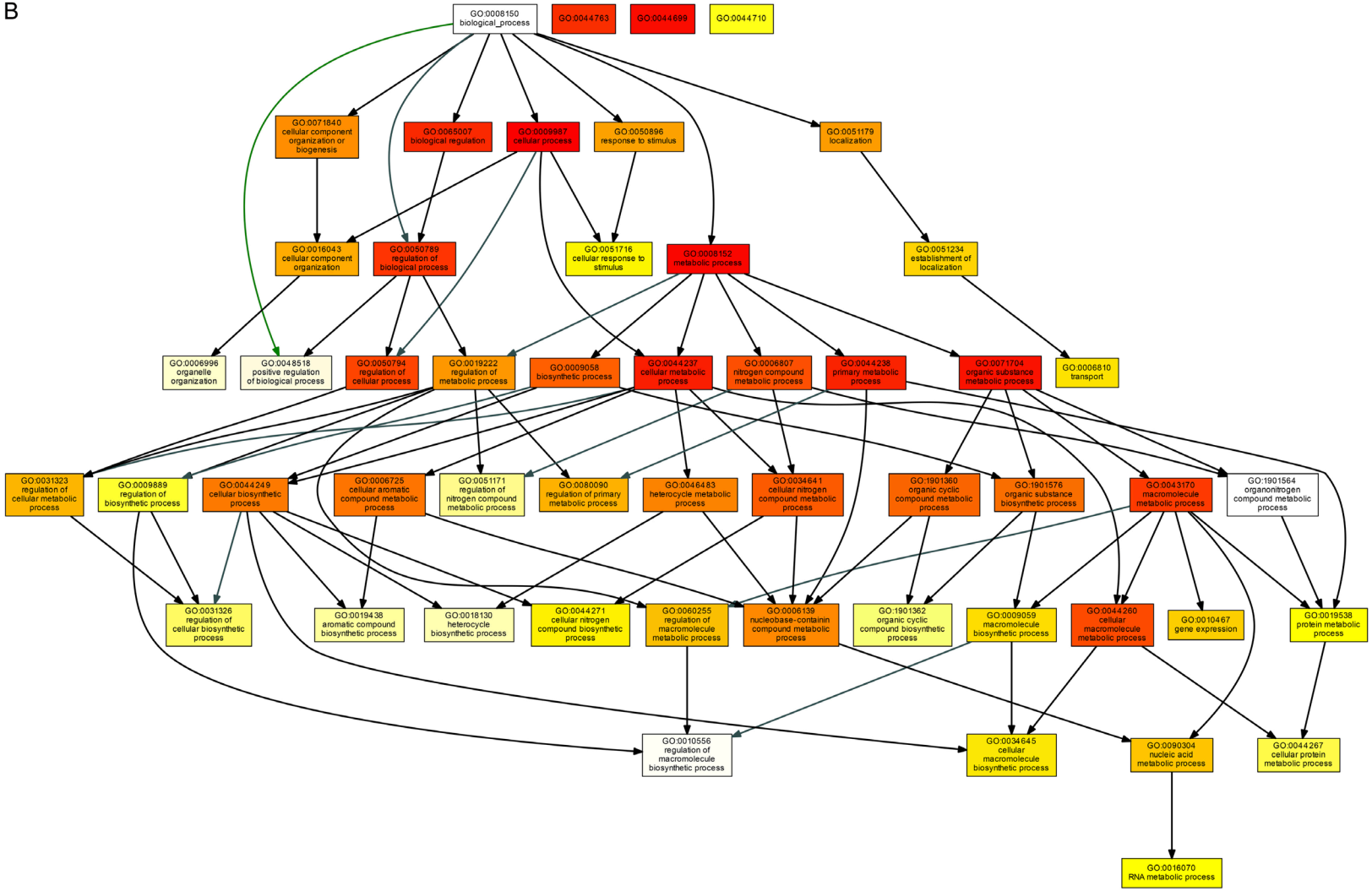
GO:0008150 biological_process
GO:0044763
GO:0044699
GO:0044710
GO:0071840 cellular component organization or biogenesis
GO:0065007 biological regulation
GO:0009987 cellular process
GO:0050896 response to stimulus
GO:0051179 localization
GO:0016043 cellular component organization
GO:0050789 regulation of biological process
GO:0051716 cellular response to stimulus
GO:0008152 metabolic process
GO:0051234 establishment of localization
GO:0006996 organelle organization
GO:0048518 positive regulation of biological process
GO:0050794 regulation of cellular process
GO:0019222 regulation of metabolic process
GO:0009058 biosynthetic process
GO:0044237 cellular metabolic process
GO:0006807 nitrogen compound metabolic process
GO:0044238 primary metabolic process
GO:0071704 organic substance metabolic process
GO:0006810 transport
GO:0031323 regulation of cellular metabolic process
GO:0009889 regulation of biosynthetic process
GO:0044249 cellular biosynthetic process
GO:0006725 cellular aromatic compound metabolic process
GO:0051171 regulation of nitrogen compound metabolic process
GO:0080090 regulation of primary metabolic process
GO:0046483 heterocycle metabolic process
GO:0034641 cellular nitrogen compound metabolic process
GO:1901360 organic cyclic compound metabolic process
GO:1901576 organic substance biosynthetic process
GO:0043170 macromolecule metabolic process
GO:1901564 organonitrogen compound metabolic process
GO:0031326 regulation of cellular biosynthetic process
GO:0019438 aromatic compound biosynthetic process
GO:0018130 heterocycle biosynthetic process
GO:0044271 cellular nitrogen compound biosynthetic process
GO:0060255 regulation of macromolecule metabolic process
GO:0006139 nucleobase-containin compound metabolic process
GO:1901362 organic cyclic compound biosynthetic process
GO:0009059 macromolecule biosynthetic process
GO:0044260 cellular macromolecule metabolic process
GO:0010467 gene expression
GO:0019538 protein metabolic process
GO:0010556 regulation of macromolecule biosynthetic process
GO:0034645 cellular macromolecule biosynthetic process
GO:0090304 nucleic acid metabolic process
GO:0044267 cellular protein metabolic process
GO:0016070 RNA metabolic process

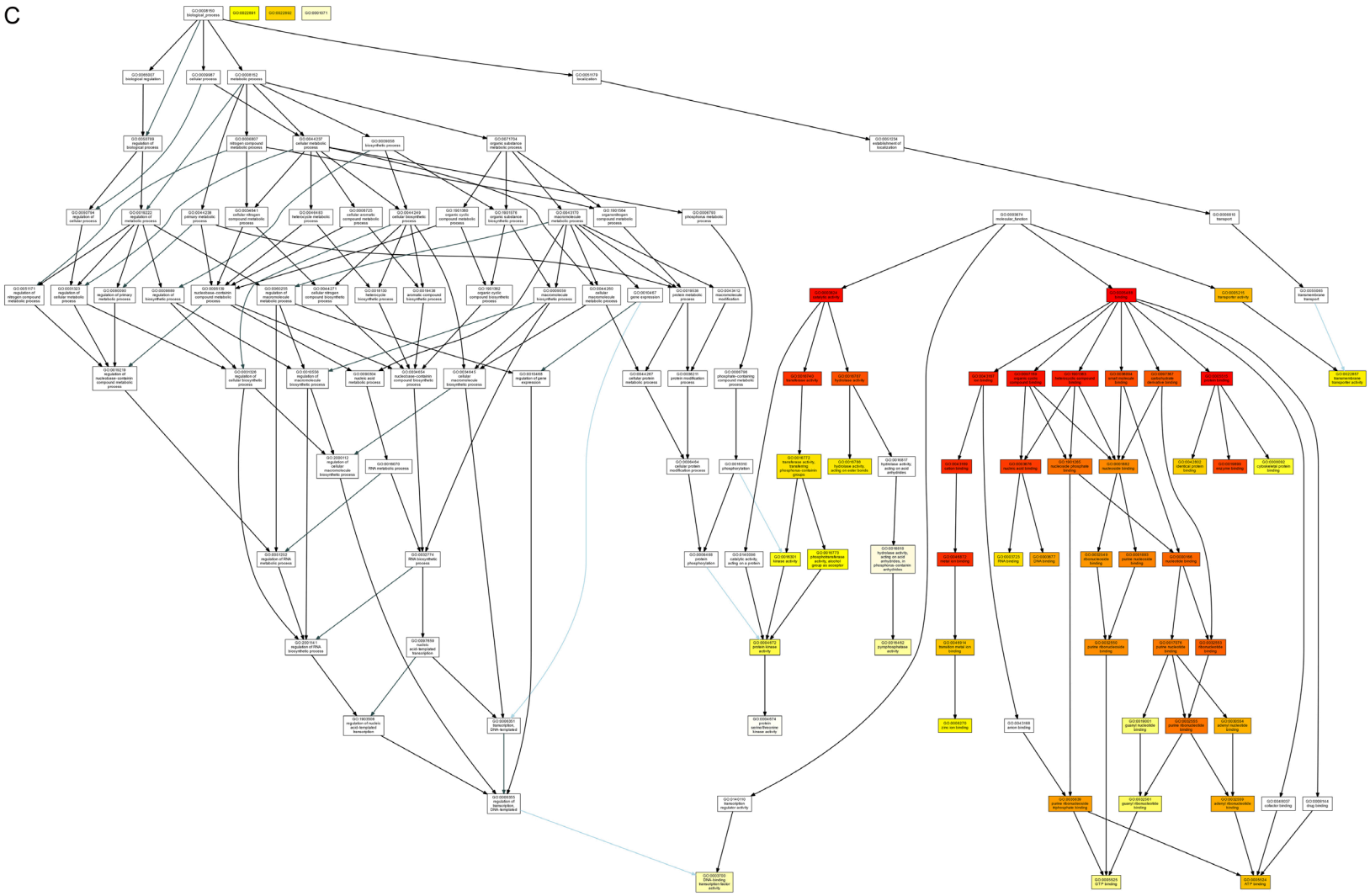

Figure 3. GO enrichment analysis of aberrantly expressed mRNAs. GO enrichment analysis cover three domains: cellular component (A), molecular function (B) and biological process (C).

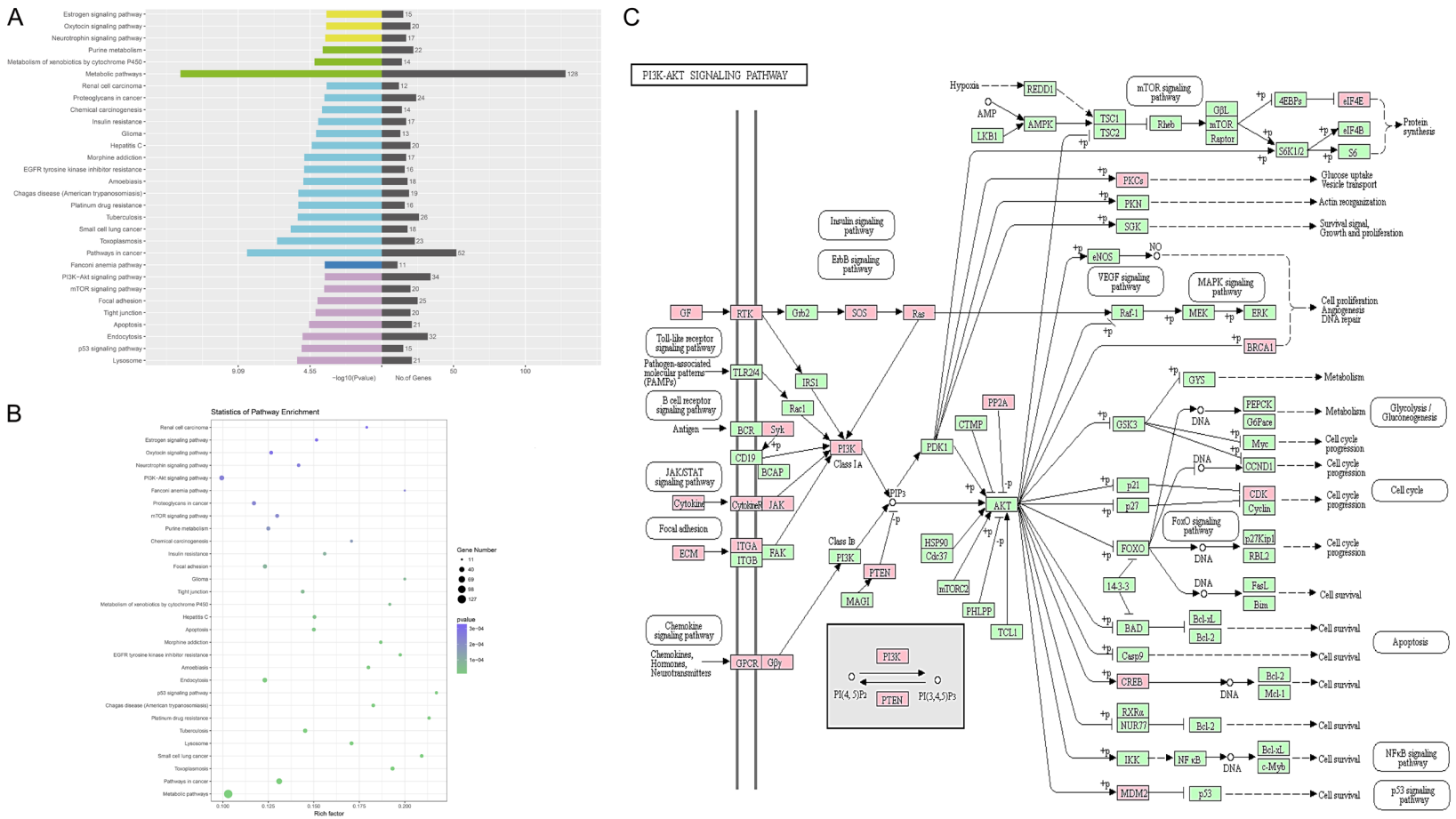

Figure 4. KEGG enrichment analysis of aberrantly expressed mRNAs. A. KEGG enrichment analysis for all aberrantly expressed lncRNAs in PE. B. Bubble diagram shows the statistics of pathway enrichment. The size of bubble means the number of genes and the color means *p*-value. C. KEGG target PI3k-Akt signaling pathway network (Background number: 342, P = 0.000248).

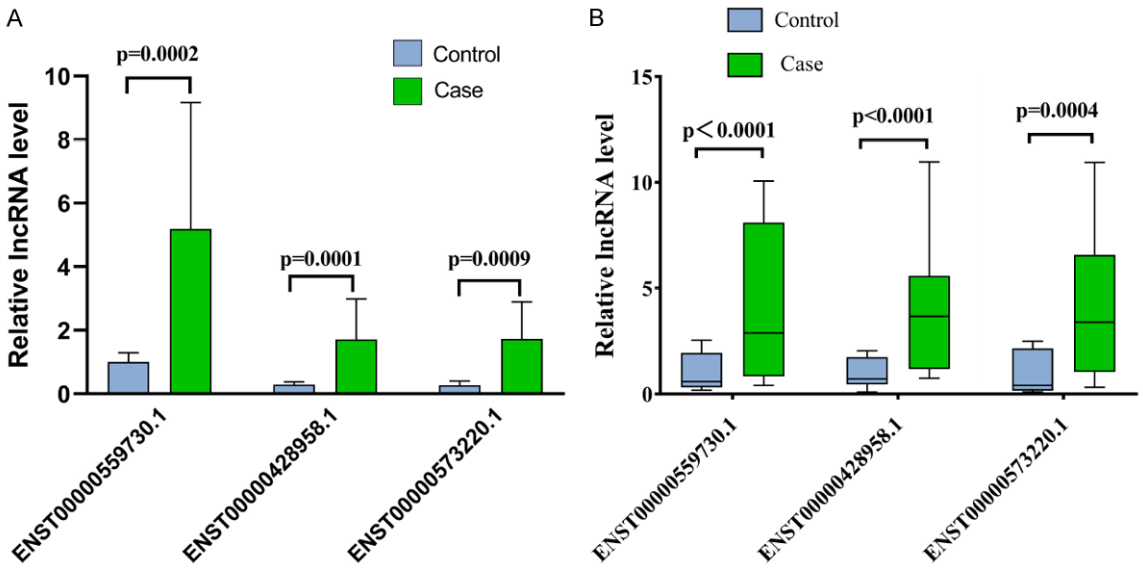

Figure 5. The results of candidate lncRNAs validation. Three candidate lncRNAs were selected according to the relative expression levels in PE and NC groups in training cohort (A). The exosomal lncRNA expression levels in PE group were significantly higher than those in NC group in validation cohort ($P < 0.001$) (B). Take cel-mir-39-3p as the external reference, and set three multiple holes each.

genic mechanism of PE and find out the target of predicting and diagnosing PE. At present, most studies on PE are based on the exosomes or lncRNAs of placental tissues. Placental tissue is difficult to obtain before parturition. In the other hand, biological fluids such as blood, urine, and saliva which are easily obtained, are more clinically practical in prenatal screening and diagnosis. In consideration of its practical use, this study objectice is to investigate the aberrantly expressed exosomal lncRNAs in PE plasmatic samples.

In PE patients, the exosomes delivered sFlt-1 and sEng to endothelial cells affect the vascular function which has proved that exosomes can reduce the migration, angiogenesis, and proliferation of human umbilical vein endothelial cells *in vitro* and provide potential intervention targets for PE [18]. Another study, which explored the volume of plasmatic total exosomes and placenta-derived exosome in maternal circulation, found that the concentrations in PE patients are significantly higher than that in NC pregnant women and exosomal miRNA, hsa-mir-486-1-5p and hsa-mir-486-2-5p, are considered to be potentially associated with PE pathogenesis [19]. This research proved strong evidence that the plasma exosomes changes and its contexts play a key role in PE pathogenesis.

During placental angiogenesis, the miRNA-related endonuclease expression is high in the perivascular chorionic membrane which suggests that miRNAs are important in placental angiogenesis and helical artery remodeling [20]. Many miRNAs are specifically expressed during pregnancy. The miRNA cluster of human chromosome 19 (C19MC) is the largest known miRNA cluster so far, including 46 miRNA clusters. It is also the most abundant miRNA species in trophoblast cell exosomes and is specifically highly expressed in the human placenta. C19MC is highly expressed in PE patients, where miR-517b, a member of C19MC, inhibits the proliferation of placental villi cells [21]. Placental mesenchymal stem cells under hypoxic conditions produced exosomes to promote angiogenesis and migration of placental microvascular endothelial cells [3]. Exosomal miR-214 which is secreted by human microvascular endothelial cells promotes proliferation, migration, and invasion of trophoblast cells [22]. Exosomes in peripheral blood plasma of healthy pregnant women facilitate the migration of human umbilical vein endothelial cells (HUVECs), meanwhile, in PE patients, the elevated expression of miR-16 inhibited HUVECs results in the formation of blood vessels and the migration of trophoblast cells [23].

Exosomal expression profiles changes in PE patients can variously affect the pathogenesis.

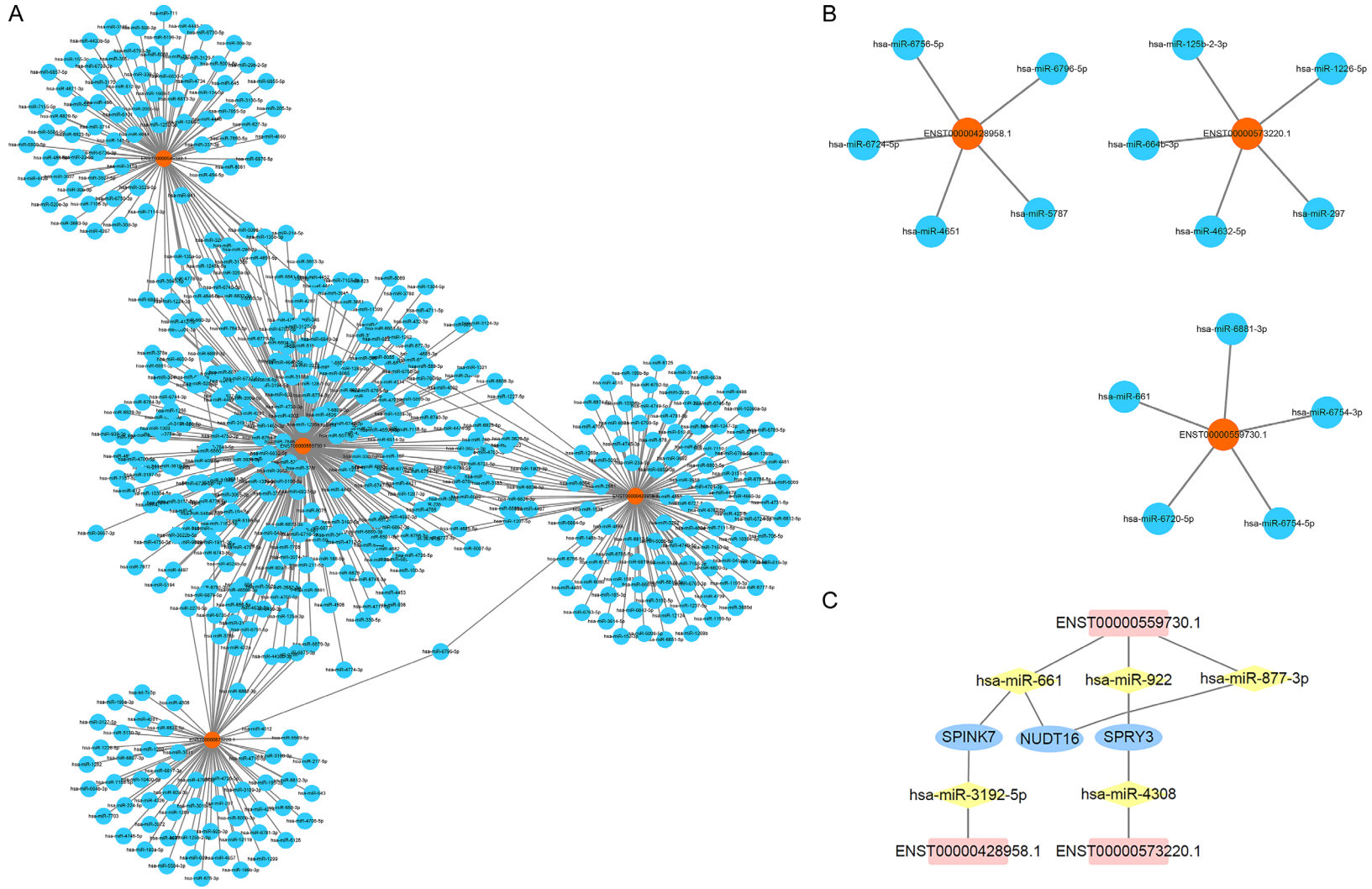

Figure 6. lncRNA-miRNA-mRNA co-expression network construction. A. Coexpression lncRNA-miRNA network shows the potential relationship between aberrantly expressed miRNAs and lncRNAs. B. Coexpression lncRNA-miRNA (Top 5) network. C. lncRNA-miRNA-mRNA coexpression network of ENST00000559730-hsa-miR-661-NUDT16.

Although the expression and biological function of lncRNAs in the placenta is still not clear, lncRNA has become a research focus in recent years due to its role in the regulation of DNA methylation, apoptosis, and angiogenesis. More and more lncRNA species are associated with placental development and PE. SPRY4-IT1, a type of lncRNA, expression is higher in PE patients' placental tissue than in normal pregnant women [24]. However, in the study of the relationship between placental implantation and PE, the lncRNA, and MALAT1, showed contradiction in function. Chen's results [25] indicates that the expression level of MALAT1 in the placenta of preeclampsia patients was significantly reduced compared with the placental implantation group. Whereas Tseng [26] found that the expression level of MALAT1 was high in the placenta of patients with placental implantation. It is obvious that MALAT1 expression affects the invasion and migration of trophoblastic cells. However, the differential expression of MALAT1 was only shown after trophoblastic invasion [27]. Therefore, the change of MALAT1 as a marker of trophoblastic invasion still needs further study. Li results showed lncRNA gastric carcinoma high expressed transcript 1 (GHET1) affects the mechanism in the development of preeclampsia [28].

In this study, we found that there were 289 significantly differential expression of lncRNAs in plasma exosomes between the PE group and the NC group, among which 155 were significantly up-regulated and 134 were significantly down-regulated. Three candidate lncRNAs were selected according to the fold change and the significance level, and qRT-PCR was performed for the significant differences verification between the two groups. The Human Body Map and NCBI GEO database search was performed and the finding showed that ENST00000559730.1 was expressed in multiple human organs, especially in the placenta (FPKM = 1.017), plasmatic exosome (FPKM = 21.7709) and HUVEC exosome (FPKM = 57.3301). ENST00000573220.1 was expressed highly in testis and thyroid, a small amount in the placenta. ENST00000428958.1 expressed only in testis, negative in exosomes. Currently, there are few reports about the aforementioned three lncRNAs thus further works will focus on the verification in exosome and intracellular level to improve the research in exploring the related signaling pathways effects on PE.

In order to further understand the function of these 289 differential expression of lncRNAs that are closely related to the pathogenesis of PE, we predicted the target genes and performed functional analyzed through KEGG and GO network. KEGG pathway analysis showed that target mRNAs were enriched in 290 signaling pathways, in which 159 pathways with $P < 0.05$ were mainly enriched in the metabolic pathway, cancer pathway, and PI3K-Akt signaling pathway. Our analysis showed that cancer pathway is closely related to metabolic and inflammatory diseases. Focusing on tumor, metabolic and inflammatory pathways, we provide new targets and strategies for the PE treatment. The metabolic pathway and PI3K-Akt signaling pathway is supposedly related to PE. PI3K-Akt signaling pathway is a signal transduction pathway that plays an important regulatory role in endothelial cells through phosphorylation or dephosphorylation, especially in angiogenesis. PI3K/Akt/eNOS pathway produces NO by mobilizing endothelial progenitor cells. In this pathway, activated Akt induces endothelial nitric oxide synthase (eNOS) which is distributed in the vascular endothelium to release of nitric oxide (NO) [29]. As an endogenous vasodilator, NO has the effects of relaxing vascular smooth muscle cells, inhibiting platelet activation, promoting angiogenesis, and increasing vascular permeability. In our previous study, we have found that NO protects vascular endothelial cells in patients with gestational hypertension [30]. In PE there is a unique eNOS signaling pathway in the vascular endothelial cells, which eventually leads to eNOS activation and NO production [31]. Angiogenesis is the foundation of trophoblast cell invasion, helical artery dilatation, capillary network formation, and vascular recasting which plays a very important role in improving the receptivity of endometrium.

The lncRNA-miRNA-mRNA co-expression network was constructed by bioinformatic analysis and it was able to identify that lncRNA ENST00000559730-hsa-miR-661-NUDT16 as the one with the most significantly differential. ENST00000559730 is an unknown lncRNA that has not been reported yet. Furthermore, Human NUDT16 is a member of Nudix hydrolase family which consists of typical (d) NTPs,

oxidized (d) NTPs, non-nucleoside polyphosphate, and capped mRNA. NUDT16 regulate the stability of 53BP1 in the progress of normal growth and DNA damage to affect the DNA repairing [32].

Conclusions

Our study not only improves the understanding of the occurrence and development of PE, but also provides new insight in the exploration of PE pathogenesis, and provides new targets for the prevention and treatment of PE. Based on previous studies and our recent results, we hypothesize that: ENST000559730, hsa-miR-661, NUDT16 affects placental angiogenesis through a variety of signaling pathways, which leads to PE. Our study showed how the mechanism of lncRNA affecting angiogenesis. It is important to further study the effect of lncRNA miRNA co-expression network on endothelial cells, and to explore the role of exogenous lncRNA in the pathogenesis of PE. Preliminary bioinformatic findings in this study can be use to identify PE markers in plasma, thus future studies with increased sample size is necessary to verify the function of lncRNA *in vitro*.

Acknowledgements

This work was supported by the National Natural Science Foundation of China (grant number 82160295), the Natural Science Foundation of Guangxi (grant number 2018JJB140171, 2020GXNSFBA999007 and 2021GXNSFAA196018), Development and Application of Appropriate Medical and Health Technologies in Guangxi (grant number S2018111), Self-funded Project of Guangxi Health Commission (grant number Z20190512), State Scholarship Fund from China Scholarship Council (grant number 201808455037) and the Research Capacity Improvement Project of College Teacher in Guangxi (grant number 2020KY03026), the Key Research and Development Plan of Science and Technology Project in Qingxiu District in Nanning City (grant number 2020054), and Medical Excellence Award Funded by the Creative Research Development Grant from the First Affiliated Hospital of Guangxi Medical University (2020, 2021).

Disclosure of conflict of interest

None.

Address correspondence to: Yachang Zeng, Department of Obstetrics and Gynecology, The First Affiliated Hospital of Guangxi Medical University, No. 6 Shuang Yong Road, Nanning 530021, Guangxi, China. Tel: +86-0771-5356697; Fax: +86-0771-5356697; E-mail: yachang_z@sina.com; zengyachang@163.com

References

[1] Craici IM, Wagner SJ, Weissgerber TL, Grande JP and Garovic VD. Advances in the pathophysiology of pre-eclampsia and related podocyte injury. Kidney Int 2014; 86: 275-285.

[2] Burton GJ, Redman CW, Roberts JM and Moffett A. Pre-eclampsia: pathophysiology and clinical implications. BMJ 2019; 366: 12381.

[3] Salomon C, Torres MJ, Kobayashi M, Scholz-Romero K, Sobrevia L, Dobierzewska A, Illanes SE, Mitchell MD and Rice GE. A gestational profile of placental exosomes in maternal plasma and their effects on endothelial cell migration. PLoS One 2014; 9: e98667.

[4] Salomon C and Rice GE. Role of exosomes in placental homeostasis and pregnancy disorders. Prog Mol Biol Transl Sci 2017; 145: 163-179.

[5] Zhao G, Yang C, Yang J, Liu P, Jiang K, Shaukat A, Wu H and Deng G. Placental exosome-mediated Bta-miR-499-Lin28B/let-7 axis regulates inflammatory bias during early pregnancy. Cell Death Dis 2018; 9: 704.

[6] Zhang Y and Zhang M. lncRNA SNHG14 involved in trophoblast cell proliferation, migration, invasion and epithelial-mesenchymal transition by targeting miR-330-5p in pre-eclampsia. Zygote 2020; 29: 108-117.

[7] Zhou F, Sun Y, Chi Z, Gao Q and Wang H. Long noncoding RNA SNHG12 promotes the proliferation, migration, and invasion of trophoblast cells by regulating the epithelial-mesenchymal transition and cell cycle. J Int Med Res 2020; 48: 300060520922339.

[8] Luo X and Li X. Long non-coding RNAs serve as diagnostic biomarkers of preeclampsia and modulate migration and invasiveness of trophoblast cells. Med Sci Monit 2018; 24: 84-91.

[9] Wang N, Li R and Xue M. Potential regulatory network in the PSG10P/miR-19a-3p/IL1RAP pathway is possibly involved in preeclampsia pathogenesis. J Cell Mol Med 2019; 23: 852-864.

[10] Wu HY, Wang XH, Liu K and Zhang JL. LncRNA MALAT1 regulates trophoblast cells migration and invasion via miR-206/IGF-1 axis. Cell Cycle 2020; 19: 39-52.

[11] Arulkumaran S, Ledger W, Denny L, Doumouchtsis S, Magee LA and von Dadelszen P.

Hypertension. In: Arulkumaran S, Ledger W, Denny L, Doumouchtsis S, editors. Oxford Textbook of Obstetrics and Gynaecology. United Kingdom: Oxford University Press; 2020. pp. 268-283.

[12] Witwer KW, Buzás EI, Bemis LT, Bora A, Lässer C, Lötvall J, Nolte-'t Hoen EN, Piper MG, Sivaraman S, Skog J, Théry C, Wauben MH and Hochberg F. Standardization of sample collection, isolation and analysis methods in extracellular vesicle research. J Extracell Vesicles 2013; 2.

[13] Théry C, Witwer KW, Aikawa E, Alcaraz MJ, Anderson JD, Andriantsitohaina R, Antoniou A, Arab T, Archer F, Atkin-Smith GK, Ayre DC, Bach JM, Bachurski D, Baharvand H, Balaj L, Baldacchino S, Bauer NN, Baxter AA, Bebawy M, Beckham C, Bedina Zavec A, Benmoussa A, Berardi AC, Bergese P, Bielska E, Blenkiron C, Bobis-Wozowicz S, Boilard E, Boireau W, Bongiovanni A, Borràs FE, Bosch S, Boulanger CM, Breakefield X, Breglio AM, Brennan MÁ, Brigstock DR, Brisson A, Broekman ML, Bromberg JF, Bryl-Górecka P, Buch S, Buck AH, Burger D, Busatto S, Buschmann D, Bussolati B, Buzás EI, Byrd JB, Camussi G, Carter DR, Caruso S, Chamley LW, Chang YT, Chen C, Chen S, Cheng L, Chin AR, Clayton A, Clerici SP, Cocks A, Cocucci E, Coffey RJ, Cordeiro-da-Silva A, Couch Y, Coumans FA, Coyle B, Crescitelli R, Criado MF, D'Souza-Schorey C, Das S, Datta Chaudhuri A, de Candia P, De Santana EF, De Wever O, Del Portillo HA, Demaret T, Deville S, Devitt A, Dhondt B, Di Vizio D, Dieterich LC, Dolo V, Dominguez Rubio AP, Dominici M, Dourado MR, Driedonks TA, Duarte FV, Duncan HM, Eichenberger RM, Ekström K, El Andaloussi S, Elie-Caille C, Erdbrügger U, Falcón-Pérez JM, Fatima F, Fish JE, Flores-Bellver M, Försönits A, Frelet-Barrand A, Fricke F, Fuhrmann G, Gabrielsson S, Gámez-Valero A, Gardiner C, Gärtner K, Gaudin R, Gho YS, Giebel B, Gilbert C, Gimona M, Giusti I, Goberdhan DC, Görgens A, Gorski SM, Greening DW, Gross JC, Gualerzi A, Gupta GN, Gustafson D, Handberg A, Haraszti RA, Harrison P, Hegyesi H, Hendrix A, Hill AF, Hochberg FH, Hoffmann KF, Holder B, Holthofer H, Hosseinkhani B, Hu G, Huang Y, Huber V, Hunt S, Ibrahim AG, Ikezu T, Inal JM, Isin M, Ivanova A, Jackson HK, Jacobsen S, Jay SM, Jayachandran M, Jenster G, Jiang L, Johnson SM, Jones JC, Jong A, Jovanovic-Talisman T, Jung S, Kalluri R, Kano SI, Kaur S, Kawamura Y, Keller ET, Khamari D, Khomyakova E, Khvorova A, Kierulf P, Kim KP, Kislinger T, Klingeborn M, Klinke DJ 2nd, Kornek M, Kosanović MM, Kovács ÁF, Krämer-Albers EM, Krasemann S, Krause M, Kurochkin IV, Kusuma GD, Kuypers S, Laitinen S, Langevin SM, Languino LR, Lannigan J, Lässer C, Laurent LC, Lavieu G, Lázaro-Ibáñez E, Le Lay S, Lee MS, Lee YXF, Lemos DS, Lenassi M, Leszczynska A, Li IT, Liao K, Libregts SF, Ligeti E, Lim R, Lim SK, Linē A, Linnemannstöns K, Llorente A, Lombard CA, Lorenowicz MJ, Lörincz ÁM, Lötvall J, Lovett J, Lowry MC, Loyer X, Lu Q, Lukomska B, Lunavat TR, Maas SL, Malhi H, Marcilla A, Mariani J, Mariscal J, Martens-Uzunova ES, Martin-Jaular L, Martinez MC, Martins VR, Mathieu M, Mathivanan S, Maugeri M, McGinnis LK, McVey MJ, Meckes DG Jr, Meehan KL, Mertens I, Minciacchi VR, Möller A, Møller Jørgensen M, Morales-Kastresana A, Morhayim J, Mullier F, Muraca M, Musante L, Mussack V, Muth DC, Myburgh KH, Najrana T, Nawaz M, Nazarenko I, Nejsum P, Neri C, Neri T, Nieuwland R, Nimrichter L, Nolan JP, Nolte-'t Hoen EN, Noren Hooten N, O'Driscoll L, O'Grady T, O'Loghlen A, Ochiya T, Olivier M, Ortiz A, Ortiz LA, Osteikoetxea X, Østergaard O, Ostrowski M, Park J, Pegtel DM, Peinado H, Perut F, Pfaffl MW, Phinney DG, Pieters BC, Pink RC, Pisetsky DS, Pogge von Strandmann E, Polakovicova I, Poon IK, Powell BH, Prada I, Pulliam L, Quesenberry P, Radeghieri A, Raffai RL, Raimondo S, Rak J, Ramirez MI, Raposo G, Rayyan MS, Regev-Rudzki N, Ricklefs FL, Robbins PD, Roberts DD, Rodrigues SC, Rohde E, Rome S, Rouschop KM, Rughetti A, Russell AE, Saá P, Sahoo S, Salas-Huenuleo E, Sánchez C, Saugstad JA, Saul MJ, Schiffelers RM, Schneider R, Schøyen TH, Scott A, Shahaj E, Sharma S, Shatnyeva O, Shekari F, Shelke GV, Shetty AK, Shiba K, Siljander PR, Silva AM, Skowronek A, Snyder OL 2nd, Soares RP, Sódar BW, Soekmadji C, Sotillo J, Stahl PD, Stoorvogel W, Stott SL, Strasser EF, Swift S, Tahara H, Tewari M, Timms K, Tiwari S, Tixeira R, Tkach M, Toh WS, Tomasini R, Torrecilhas AC, Tosar JP, Toxavidis V, Urbanelli L, Vader P, van Balkom BW, van der Grein SG, Van Deun J, van Herwijnen MJ, Van Keuren-Jensen K, van Niel G, van Royen ME, van Wijnen AJ, Vasconcelos MH, Vechetti IJ Jr, Veit TD, Vella LJ, Velot É, Verweij FJ, Vestad B, Viñas JL, Visnovitz T, Vukman KV, Wahlgren J, Watson DC, Wauben MH, Weaver A, Webber JP, Weber V, Wehman AM, Weiss DJ, Welsh JA, Wendt S, Wheelock AM, Wiener Z, Witte L, Wolfram J, Xagorari A, Xander P, Xu J, Yan X, Yáñez-Mó M, Yin H, Yuana Y, Zappulli V, Zarubova J, Žėkas V, Zhang JY, Zhao Z, Zheng L, Zheutlin AR, Zickler AM, Zimmermann P, Zivkovic AM, Zocco D and Zuba-Surma EK. Minimal information for studies of extracellular vesicles 2018 (MISEV2018): a position statement of the International Society for Extracellular Vesicles and update of the MISEV2014 guidelines. J Extracell Vesicles 2018; 7: 1535750.

[14] Yuana Y, Böing AN, Grootemaat AE, van der Pol E, Hau CM, Cizmar P, Buhr E, Sturk A and Nieuwland R. Handling and storage of human body fluids for analysis of extracellular vesicles. J Extracell Vesicles 2015; 4: 29260.
[15] Redman CW, Sargent IL and Staff AC. IFPA Senior Award Lecture: making sense of pre-eclampsia - two placental causes of preeclampsia? Placenta 2014; 35 Suppl: S20-25.
[16] Repiska G, Konecna B, Shelke GV, Lasser C, Vlkova BI and Minarik G. Is the DNA of placental origin packaged in exosomes isolated from plasma and serum of pregnant women? Clin Chem Lab Med 2018; 56: e150-e153.
[17] Gadde R, Cd D and Sheela SR. Placental protein 13: an important biological protein in preeclampsia. J Circ Biomark 2018; 7: 184-189.
[18] Chang X, Yao J, He Q, Liu M, Duan T and Wang K. Exosomes from women with preeclampsia induced vascular dysfunction by delivering sFlt (Soluble Fms-Like Tyrosine Kinase)-1 and sEng (Soluble Endoglin) to endothelial cells. Hypertension 2018; 72: 1381-1390.
[19] Salomon C, Guanzon D, Scholz-Romero K, Longo S, Correa P, Illanes SE and Rice GE. Placental exosomes as early biomarker of preeclampsia: potential role of exosomal microrna across gestation. J Clin Endocrinol Metab 2017; 102: 3182-3194.
[20] Forbes K, Farrokhnia F, Aplin JD and Westwood M. Dicer-dependent miRNAs provide an endogenous restraint on cytotrophoblast proliferation. Placenta 2012; 33: 581-585.
[21] Delorme-Axford E, Donker RB, Mouillet JF, Chu T, Bayer A, Ouyang Y, Wang T, Stolz DB, Sarkar SN, Morelli AE, Sadovsky Y and Coyne CB. Human placental trophoblasts confer viral resistance to recipient cells. Proc Natl Acad Sci U S A 2013; 110: 12048-12053.
[22] Gong F, Cheng H, Shi Y, Cui L and Jia G. LncRNA TDRG1/miR-214-5p axis affects preeclampsia by modulating trophoblast cells. Cell Biochem Funct 2019; 11: 16.
[23] Hu Y, Li P, Hao S, Liu L, Zhao J and Hou Y. Differential expression of microRNAs in the placentae of Chinese patients with severe pre-eclampsia. Clin Chem Lab Med 2009; 47: 923-929.
[24] Zou Y, Jiang Z, Yu X, Sun M, Zhang Y, Zuo Q, Zhou J, Yang N, Han P, Ge Z, De W and Sun L. Upregulation of long noncoding RNA SPRY4-IT1 modulates proliferation, migration, apoptosis, and network formation in trophoblast cells HTR-8SV/neo. PLoS One 2013; 8: e79598.
[25] Chen H, Meng T, Liu X, Sun M, Tong C, Liu J, Wang H and Du J. Long non-coding RNA MALAT-1 is downregulated in preeclampsia and regulates proliferation, apoptosis, migration and invasion of JEG-3 trophoblast cells. Int J Clin Exp Pathol 2015; 8: 12718-12727.
[26] Tseng JJ, Hsieh YT, Hsu SL and Chou MM. Metastasis associated lung adenocarcinoma transcript 1 is up-regulated in placenta previa increta/percreta and strongly associated with trophoblast-like cell invasion in vitro. Mol Hum Reprod 2009; 15: 725-731.
[27] Li X, Song Y, Liu F, Liu D, Miao H, Ren J, Xu J, Ding L, Hu Y, Wang Z, Hou Y and Zhao G. Long non-coding RNA MALAT1 promotes proliferation, angiogenesis, and immunosuppressive properties of mesenchymal stem cells by inducing VEGF and IDO. J Cell Biochem 2017; 118: 2780-2791.
[28] Li S, Liu J, Kong F, Wang Y, Li N and Zou Y. lncRNA GHET1 has effects in development of pre-eclampsia. J Cell Biochem 2019; 120: 12647-12652.
[29] Siragusa M and Fleming I. The eNOS signalosome and its link to endothelial dysfunction. Pflugers Arch 2016; 468: 1125-1137.
[30] Zeng Y, Li M, Chen Y and Wang S. Homocysteine, endothelin-1 and nitric oxide in patients with hypertensive disorders complicating pregnancy. Int J Clin Exp Pathol 2015; 8: 15275-15279.
[31] Ma RQ, Sun MN and Yang Z. Effects of pre-eclampsia-like symptoms at early gestational stage on feto-placental outcomes in a mouse model. Chin Med J (Engl) 2010; 123: 707-712.
[32] Zhang F, Lou L, Peng B, Song X, Reizes O, Almasan A and Gong Z. Nudix hydrolase NUDT16 regulates 53BP1 protein by reversing 53BP1 ADP-ribosylation. Cancer Res 2020; 80: 999-1010.